Colloids and Surfaces B: Biointerfaces 164 (2018) 262–271

Contents lists available at ScienceDirect

Colloids and Surfaces B: Biointerfaces

journal homepage: www.elsevier.com/locate/colsurfb

Two-step biocompatible surface functionalization for two-pathway antimicrobial action against Gram-positive bacteria

Diego E. Pissinis, Guillermo A. Benítez, Patricia L. Schilardi*

Instituto de Investigaciones Fisicoquímicas Teóricas y Aplicadas (INIFTA), CONICET- Facultad de Ciencias Exactas, Universidad Nacional de La Plata, Casilla de Correo 16, Sucursal 4, 1900, La Plata, Argentina

ARTICLE INFO

Article history:
Received 24 October 2017
Received in revised form 14 January 2018
Accepted 28 January 2018
Available online 31 January 2018

Keywords:
Antibacterial
Surface functionalization
Silver nanoparticles
Ampicillin

ABSTRACT

The use of indwelling devices has emerged as a frequent and often life-saving medical procedure. However, infection in prosthetic surgery is one of the most important and devastating complications. Once the biofilm has been formed, its eradication is extremely difficult, due to an increased resistance to host defense and conventional antimicrobials. Thus, the design of novel strategies for inhibiting the bacterial adhesion on implantable devices is a key point for successful surgical procedures. In this work, the development of a simple two-step protocol to prepare surfaces able to prevent the bacterial growth was successfully achieved. The surface-modification design includes a combined approach involving the multi-functionalization of Ti surfaces with silver nanoparticles (AgNPs) and/or ampicillin (AMP). The surface chemistry involved in AMP adsorption on titanium and silver surfaces was elucidated for the first time, thus establishing the basis for the further anchoring of other antibacterial compounds having similar functional groups. Our results show that the antibiotic binds to the titanium surface through covalent interactions between the —COOH groups in AMP and the —OH groups of the native TiO_2 on the surface, although electrostatic interactions between protonated AMP and negatively charged TiO_2 can also contribute to the antibiotic anchoring to the surface. The AMP immobilization on the AgNPs is carried out by thiolate-like bonds. The β-lactam ring functionality is preserved after the adsorption process, since the Ti-AgNPs-AMP surface was able to decrease the bacterial viability in more than 80%. Moreover, the antimicrobial capacity is maintained over time due to a two-pathway antibacterial mechanism: death by contact (AMP) and death by release (AgNPs). The effect of AMP prevails on AgNPs at early stages of bacterial adhesion, while AgNPs are responsible for sustaining the relatively low but steady release of Ag(I), preserving the bacteriostatic activity of the surface over time. This effect would contribute to prevent infections due to sessile cells on indwelling devices, powering the action of the immune system and the conventional antibiotics usually dosed in implanted patients.

1. Introduction

The use of indwelling devices has emerged as a frequent and often life-saving medical procedure. However, infection in prosthetic surgery is one of the most important and devastating complications [1]. Its incidence is about 2–3% in primary prosthesis and twice in revision surgeries, reaching percentages above 15% in constrained or hinged implants [2]. The infection may be originated from bacteria already present in the individual or from those that entered by contamination of the material or improper handling during the surgical procedure. Once the biofilm has been formed, its eradication is extremely difficult due to an increased resistance to host defense and conventional antimicrobials. This resistive mechanism comprises: (i) protection of internal cells from aggressive environments and, in the case of prostheses, from the host immune system; (ii) creation of a diffusional barrier to large molecules or the entrapment of antibacterial substances and (iii) reduction in metabolic rate and induction of oxygen gradients across the biofilm, which contribute to the phenotypic heterogeneity within the bacterial population [3]. It is also important to highlight that, in conventional treatments, the antimicrobial agent acts effectively on the outer part of the biofilm (rapidly growing cells) and hardly on the region adjacent to the surface of the biomaterial (stressed cells or persisters). Bacterial strategies also involve a high cell density, which minimizes both the area exposed

* Corresponding author.
E-mail addresses: dpissinis@inifta.unlp.edu.ar (D.E. Pissinis), gbenitez@inifta.unlp.edu.ar (G.A. Benítez), pls@inifta.unlp.edu.ar, patricia.schilardi@gmail.com (P.L. Schilardi).

https://doi.org/10.1016/j.colsurfb.2018.01.057
0927-7765/

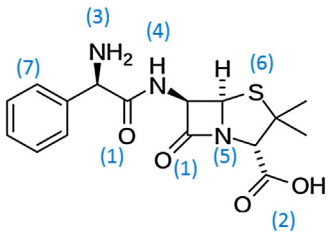

Fig. 1. Chemical structure of ampicillin. The functional groups are labeled: (1) carbonyl; (2) carboxyl; (3) primary amine; (4) amide; (5) lactam; (6) sulfide; (7) aromatic.

to the aggressive environment and the sacrifice of microbes that are directly exposed to the antimicrobial agent [4]. Therefore, an effective strategy to enhance the antimicrobial action and to inhibit the development of biofilms is the prevention of the formation of two- or three-dimensional compact layers of bacteria, which can be done by the proper modification of the surface chemistry. For instance, for this aim, the antimicrobials adsorption on polymeric surfaces has already been explored: polytetrafluoroethylene (PTFE) modified by penicillin [5,6] and ampicillin (AMP) [7], amoxicillin on poly(dimethylsiloxane) (PDMS) surfaces [8], etc. These antibiotics belong to the β-lactam family, which binds to penicillin-binding proteins (PBPs) which are responsible for the cross-linking of peptidoglycan in the cell wall synthesis. In this process, the β-lactam ring (Fig. 1) reacts with these enzymes to form stable covalent complexes, leading to inactivation of the PBPs and ultimately to cell death. These covalent complexes are formed as a result of the covalent binding of —OH group in the enzyme and the carbonyl group from the β-lactam ring after the cleavage of the N—CO bond [9].

The molecular structure of ampicillin (Fig. 1) shows several functional groups which are potentially adequate for the anchoring of AMP to surfaces. Self-assembled monolayers (SAMs) of $R\text{-}COO^-$/RCOOH type compounds can be easily formed on oxidized surfaces such as $\alpha\text{-}Al_2O_3$, Fe_xO_y and TiO_2, while organosulfur compounds, including alkanethiols, dialkylsulfides and thiophenes are suitable for SAMs formation on varied metallic surfaces (Au, Ag, Cu, etc.) [10]. Thus, AMP seems to be a good candidate for the chemical modification of several surfaces in order to confer them antimicrobial characteristics, since, *a priori*, the β-lactam ring is not involved in the surface reaction and, thus, would keep its antimicrobial function.

On the other hand, the increasing resistance of microorganisms to antibiotic is a matter of great concern worldwide [11]. Therefore, the search for new strategies for the inhibition of the bacterial proliferation is in continuous progress. In view of the fact that microbes have not been able to develop resistance to silver yet, the use of silver nanoparticles (AgNPs), as relatively new antibacterial agents, has been widely studied [12–15]. The mechanism involving the antimicrobial activity of AgNPs is controversial [16] and it is still under discussion: some studies suggest that the nanoparticles interact directly with the cell wall, whereas some others attribute the antibacterial effect to Ag(I) ions release from the nanoparticles. There are authors who also postulate the combined action of both effects [17–26]. What is certainly involved is Ag(I) ions release from the AgNPs. These Ag(I) ions either interact with bacterial proteins through thiol groups [27] or affect the respiratory chain [19], and even interfere in DNA replication [24,28]. Furthermore, Xiu et al. [25] have reported that AgNPs *per se* did not significantly represent a direct particle-specific toxicity to bacteria, but they may only act as carriers for silver ions that then will conduct the toxic action on the bacteria.

The aim of this work is the design of surfaces having highly inhibiting efficiency for the adhesion and proliferation of bacteria through the immobilization of conventional antimicrobials (AMP) and/or nanomaterials (AgNPs). These agents have different mechanisms of action, which, when combined in a surface can, in turn, operate at different times. These characteristics would allow keeping the antimicrobial effect for longer periods when compared to AMP or AgNPs as single factors. We have chosen Ti as substrate because it is one of the most widely used in dental and orthopedic implants due to its high strength-to-weight ratio, corrosion resistance and mechanical wear, inert nature, ability for adsorbing proteins on their surface and biocompatibility, which allows the osseointegration [29], among other properties. On the other hand, on this metal, native oxide film (dense and stable anatase TiO_2) is naturally formed on the surface when it is exposed to air, leading to a spontaneous passivation of the metal [30,31]. To the best of our knowledge, there is not previous information about the performance of AMP and/or AgNPs immobilized on titanium surfaces with an exhaustive analysis of the surface chemistry involved. The mentioned surface chemistry analysis would help in the subsequent smart design of new antimicrobial surfaces with applications in medical devices.

2. Material and methods

2.1. Reagents

All solutions were prepared using ultrapure MilliQ® water. All reagents were analytical grade and used as received, without further purification: silver nitrate (Sigma Aldrich), sodium citrate (J.T. Baker), hydrogen peroxide 30% (Merck), sodium borohydride (Fluka), ampicillin (Fabra laboratory), nutrient broth and nutrient agar (Britania), disodium hydrogen phosphate (Fluka), potassium dihydrogen phosphate (Fluka), sodium chloride (Sigma Aldrich), phosphoric acid (J.T. Baker).

2.2. Silver nanoparticles preparation

AgNPs in aqueous solution were prepared following the methodology described by Frank et al. [32]. This synthesis leads to silver nanoprisms with controlled size. Briefly, the synthesis was carried out by adding these solutions in the following order: 2.0 mL of 1.25×10^{-2} M sodium citrate, 5.0 mL of 3.75×10^{-4} M silver nitrate, and 5.0 mL of 5.0×10^{-2} M hydrogen peroxide. The silver reduction was achieved by adding 2.5 mL of freshly prepared 5.0×10^{-3}M sodium borohydride under vigorously magnetic stirring. After approximately 3 min, a stable color is reached, indicating the end of the synthesis. The colloidal dispersion was then dialyzed for 2 h to eliminate the excess of reactives. The final Ag concentration in the nanoparticles dispersion is 18.38 μg/mL.

2.3. Silver nanoparticles functionalization with ampicillin

AgNPs functionalized with ampicillin (AMP) were obtained by adding AMP to the AgNPs dispersion until the AMP concentration reached 2 mM [33]. After 24 h, the resulting dispersion was centrifuged twice at 14.000 rpm for 30 min in order to remove the AMP-containing supernatant. Then, the pellet with ampicillin functionalized AgNPs (AgNPs/AMP) was re-suspended in ultrapure water and preserved in the dark at 25 °C.

2.4. Titanium surface preparation

The substrates were titanium discs (Johnson-Mathey, 99.7%) 1 cm in diameter and 0.25 mm in thickness. The substrates were first polished with abrasive paper, sonicated for 15 min, and then polished at mirror grade with 1 μm diamond paste. After that, the

substrates were sonicated in water and then in ethanol for 15 min and, finally, thoroughly rinsed and dried in air.

2.5. Titanium surfaces modification

2.5.1. AgNPs immobilization on Ti surfaces (*Ti-AgNPs*)

The Ti substrates were incubated in the AgNPs dispersion (1.84×10^{-2} mg Ag/mL) in the dark at 25 °C for 24 h, then rinsed and dried under nitrogen stream.

2.5.2. AgNPs/AMP immobilization on Ti surfaces (*Ti-AgNPs/AMP*)

The Ti substrates were incubated in the AgNPs/AMP dispersion in the dark at 25 °C for 24 h, then rinsed with MilliQ® water and dried under nitrogen stream.

2.5.3. Ti surface functionalization with AMP (*Ti-AMP*)

The Ti substrates were incubated in a 20 mM AMP solution in the dark at 25 °C for 24 h, then rinsed and dried under nitrogen stream.

2.5.4. Ti surface multi-functionalization whit AgNPs and AMP (*Ti-AgNPs-AMP*)

The Ti substrates were incubated in the AgNPs dispersion (1.84×10^{-2} mg Ag/mL) in the dark at 25 °C for 24 h, then rinsed and immersed in a 20 mM AMP solution in the dark at 25 °C for 24 h. After that, the samples were rinsed again and dried under nitrogen stream.

2.6. Electrochemical measurements

Electrochemical measurements were performed in a three-electrode electrochemical cell by using a Teq galvanostat-potentiostat. The working electrodes were silver foils chemically cleaned by immersion for 5 min in a solution containing H_2O_2 and NH_3. Then, the substrates were sonicated for 15 min in water, dried and functionalized as described below. As counter electrode and reference electrode, a platinum foil and a saturated calomel electrode (SCE) were used respectively. The electrolyte solution was 0.1 M NaOH, purged with N_2. The electrochemical assays were carried out by scanning the potential from −0.75 V to −1.5 V at 0.05 V/s in the electrolyte solution at room temperature.

The different modified-silver foils were prepared by incubation in (i) 1.25×10^{-2} M sodium citrate solution for 6 h; (ii) 20 mM ampicillin solution for 24 h in the dark at 25 °C; (iii) 1.25×10^{-2} M sodium citrate solution for 6 h and, then, in 20 mM ampicillin solution for 24 h in the dark at 25 °C. All the samples were rinsed with ultrapure water and dried with N_2 stream.

2.7. Spectroscopic and dynamic light scattering (DLS) measurements

UV–vis spectra of the silver nanoparticles dispersions were acquired with a Perkin Elmer Lambda 35 Spectrophotometer. X-ray Photoelectron Spectroscopy (XPS) measurements were performed using an Al Kα source (XR50, Specs GmbH) and a hemispherical electron energy analyzer (PHOIBOS 100, Specs GmbH) operating at 40 eV pass energy. A two-point calibration of the energy scale was performed using sputtered gold and copper samples (Au 4f7/2 binding energy (BE) = 84.00 eV; Cu 2p3/2 BE = 932.67 eV). C 1s at 285 eV was used as charging reference. A Malvern zetasizer Nano zs was used for DLS and zeta potential measurements.

2.8. Atomic force microscopy (AFM) imaging

AFM imaging was carried out by using a Nanoscope V microscope (Bruker) operating in tapping mode in air. Images were taken at a scanning rate of 1 Hz with etched silicon tips (RTESP, 215–254 kHz and 20–80 N/m).

Table 1
Simulated salivary fluid composition.

Disodium hydrogen phosphate	2.4 g/L
Potassium dihydrogen phosphate	0.2 g/L
Sodium chloride	8.0 g/L
Phosphoric acid	q.s. to pH 6.75

2.9. Silver surface concentration and silver release in simulated salivary fluid (SSF)

The surface concentration was determined by Inductively Coupled Plasma Optical Emission Spectrometry (ICP-OES) after the dissolution of the adsorbed AgNPs by immersing the substrates in a 5.0×10^{-2} M hydrogen peroxide solution, sonicated for 10 min and acidified with 2% HNO_3 solution.

SSF was prepared according to the composition given in [34] (Table 1). The amount of silver was determined by ICP-OES. To this aim, the Ti-AgNPs substrates were immersed in 12 mL of SSF for 6 h (which corresponds to three immersion cycles in culture media, see Section 2.10) or for 24 h. After that, each supernatant was acidified with 2% HNO_3 and the amount of silver in the resulting solutions was measured.

2.10. Bacteria attached to modified titanium surfaces viability

Staphylococcus aureus (*S. aureus*, ATCC 25923) was grown in nutrient broth at 37 °C in a rotary shaker (180 rpm). Then, the bacterial suspension was adjusted to 10^8 colony forming units (CFU)/mL (DO = 0.5) in fresh growth medium and used immediately.

A drop of 100 μL of the bacterial suspension was seeded onto each functionalized Ti substrate and left for 2 h at 37 °C to allow bacterial adhesion. The biofilmed substrates were gently washed by immersion in double-distilled sterile water to remove those cells that were not irreversibly attached to the surface. Bare Ti discs were used as control. The results were expressed as percentage of dead bacteria with respect to the control according to:

$$\left(1 - \frac{\text{viable bacteria on modified Ti}}{\text{viable bacteria on control Ti}}\right) \times 100$$

The number of viable sessile bacteria was determined through quantification by the serial dilution method and plate counting after the detachment of cells by sonication, according to the protocol developed in our lab [35]. In order to emulate long periods of exposition to bacterial culture, the substrates were re-utilized twice (three utilization series). At each step, the same procedure described above was followed: a drop of 100 μL of the bacterial suspension was seeded onto each functionalized Ti disk and left for 2 h at 37 °C to allow bacterial adhesion. The biofilmed substrates were gently washed by immersion in double-distilled sterile water to remove those cells that were not irreversibly attached to the surface. The number of viable cells was determined by serial dilution method and plate counting. After that, the substrates were softly rinsed again and utilized in the next cycle. At each step, a new bacterial culture was seeded onto the substrates.

3. Results and discussion

3.1. AgNPs characterization

In order to assess the formation of nanoparticles, UV–vis absorption spectroscopy is a suitable technique, since metal nanoparticles exhibit an intense absorption peak due to the surface plasmon resonance phenomenon (collective oscillation of surface electrons).

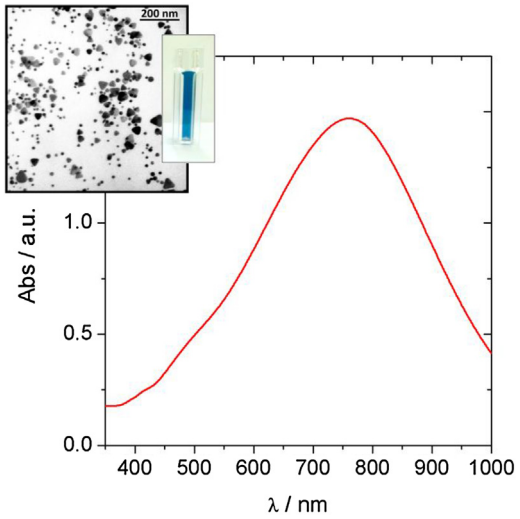

Fig. 2. UV–vis spectrum of the synthesized AgNPs in aqueous dispersion. Inset: TEM image showing the size and morphology of the AgNPs and optical image of the blue AgNPs dispersion. (For interpretation of the references to colour in this figure legend, the reader is referred to the web version of this article.)

The UV–vis absorption spectra of the citrate-capped AgNPs (Fig. 2) show a broad band at 750 nm, which is consistent with polydisperse AgNPs, as it was reported for the synthesis used in this work [32]. TEM images (Fig. 2, inset) confirm that the synthesized AgNPs consist mainly of small nanodiscs whose radius ranges from 12 to 20 nm and greater nanoprisms having 25–75 nm in lateral size. Some agglomerates, which could be formed after the drop casting of the AgNPs dispersion on the TEM grid, can also be observed. The height of these nanodiscs and nanoprisms is about 12 nm, as it was estimated by AFM after the adsorption of single nanoparticles on poly-L-lysine-modified substrates (data not shown).

3.2. Citrate by AMP exchange on citrate-capped AgNPs

AMP-functionalized AgNPs were obtained after the addition of AMP to the citrate-capped silver nanoprisms dispersion. The thioether group (labeled (6) in Fig. 1) is suitable for the adsorption of AMP on the surface. On this regard, two mechanisms might be responsible for the immobilization process: covalent interactions between AMP and the surface, such as those found for dialkylsulfides monolayers on Au(111), where C—S bonds remain after the adsorption [10]; or the chemisorption of the thiolate group after the cleavage of the C—S bond. In order to elucidate which of these interactions is responsible for the anchoring of AMP on AgNPs, we hypothesized that, if the thiolate bond is formed on Ag, the typical electrodesoption peak similar to those corresponding to alkanethiols self-assembled monolayers should be observed. Since titanium is a valve-type metal, electrochemical measurements involving AMP-capped AgNPs adsorbed on titanium electrodes are hard to carry out. Therefore, we have modified a silver foil and used it as working electrode in the voltammetric assays. Fig. 3a shows the cyclic voltammogram recorded for an Ag electrode (blank) and for citrate, AMP, and citrate followed by AMP-modified individual bulk Ag electrodes. In all runs, a cathodic peak at −0.88 V is clearly noticeable, which can be attributed to the electroreduction of some $Ag(NH_3)_2^+$ [36] remaining on the surface after the chemical cleaning of the electrodes (see experimental section). Actually, this peak is only observed in the first run when the electrode is repetitively cycled (data not shown), indicating that all the remaining silver ions are reduced in this first cycle. Furthermore, after the immersion of the electrodes in citrate or AMP solution, the charge associated to peak (I) diminishes, revealing that, in some way, part of these

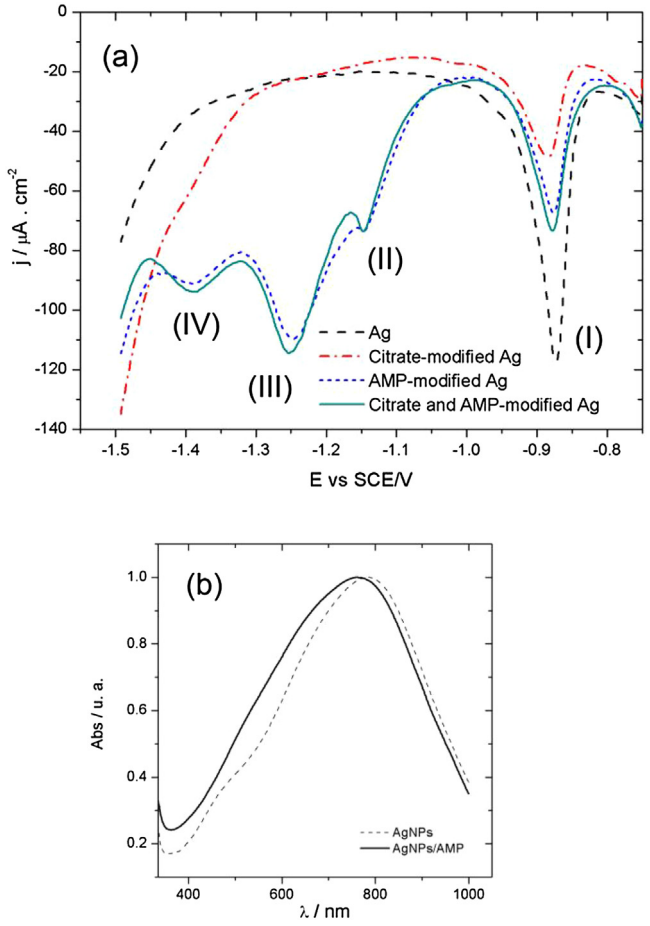

Fig. 3. (a) Voltammograms of Ag and surface-modified Ag electrodes in aqueous 0.1 M NaOH run at 0.05 V/s. (b) UV–vis spectrum of AgNPs and AgNPs/AMP.

complexes are displaced from the surface during the adsorption process. As expected, no further reduction peaks are observed for Ag and citrate-modified Ag electrodes. However, both AMP- and citrate and AMP-functionalized surfaces show three more reduction peaks located at −1.15 V, −1.26 V and −1.39 V, labeled (II), (III) and (IV), respectively, in Fig. 3a. The small peak (II) can be ascribed to little amounts of sulphur [37] due to some AMP degradation in the solution. The broad peaks (III) and (IV) are consistent with the electroreductive desorption of the chemisorbed sulphur corresponding to thiolate species. In fact, the electrodesorption of alkanethiols self-assembled monolayers on Ag(111) leads to two cathodic current peaks lying at −1.26 V and −1.38 V [38]. The first has been attributed to the removal of the alkanethiolate lattice, whereas the latter accounts for the electrodesorption of remaining thiolate on the surface. It has also been reported that thiolate electrodesorption peaks broaden on polycrystalline electrodes [39]. Thus, our results are in good agreement with those found for the electrodesorption of alkanethiolates from Ag surfaces and, therefore, peaks (III) and (IV) can be attributed to the desorption of the AMP bonded to the Ag surface through thiolate bonds. Consequently, these results indicate that the AMP adsorption on AgNPs involves the chemisorption of the S moiety on the silver surface.

The characteristic AgNPs surface plasmon resonance band shifts from 780 nm for AgNPs to 763 nm for AgNPs/AMP (Fig. 3b). This small blue-shift can be attributed to a decrease in the size of the nanoparticles, changes in the surface chemistry after functionalization or both. The mean hydrodynamic size, measured by DLS, resulted in 50 ± 29 nm and 58 ± 32 nm for AgNPs and AgNPs/AMP, respectively. The high standard deviation for these values is related

to the high polydispersity of the nanoparticles, which is intrinsic in our system. Thus, although after capping exchange, a change from blue to violet in the color of the dispersion was observed, variations in the nanoparticles size cannot be confirmed. On the other hand, z-potential measurements lead to -35.3 ± 0.2 mV and -28.0 ± 0.1 mV for AgNPs and AgNPs-AMP, respectively. The increase in the z potential value after the functionalization is consistent with the incorporation of positively charged molecules on the surface, such as the zwitterionic form of AMP. Thus, from these results, the small blue-shift in the UV–vis spectra can be attributed to changes in the surface chemistry of the nanoparticles, although variations in the nanoparticle size might also contribute to this blue-shift.

3.3. Ti/TiO_2 surfaces functionalization

In order to analyze the most effective surface to inhibit the bacterial proliferation, the substrates were modified in the following way: (1) AMP adsorption onthe Ti/TiO_2 surface; (2) AgNPs immobilization onthe Ti/TiO_2 surface; (3) AgNPs/AMP immobilization onthe Ti/TiO_2 surface; and (4) AgNPs immobilization followed by AMP adsorption onthe AgNPs-modified Ti/TiO_2 surface (multi-functionalized Ti/TiO_2 surface). The resulting substrates were characterized as described below.

3.3.1. AMP adsorption on Ti/TiO_2

The AMP-functionalized substrates (Ti/TiO_2-AMP) were evaluated by XPS by analyzing the O 1s, N 1s and S 2p signals (Fig. 4). The O 1s core level peak (Fig. 4a) can be described as resulting from three contributions at 530.5, 531.6 and 533.2 eV. These contributions can be assigned in the following way [40]: the low binding energy component at 530.5 eV is attributed to $O^{=}$ in the titanium dioxide; while 531.6 and 533.2 eV correspond to —OH and oxide and C—O and O—C=O, respectively. It is well-known that carboxylic acids adsorb on oxide-covered surfaces [41,42] forming surface complexes [43]. These strong interactions have been described as responsible for the high stability of citrate-capped AgNPs adsorbed on oxidized titanium surfaces [44]. Therefore, it is reasonable to assume that the AMP molecule is chemisorbed on the Ti/TiO_2 substrates through the formation of such surface complexes between the carboxylic group (labeled (2) in Fig. 1) and the oxidized Ti surface.

The N 1s spectrum can be fitted with three components at 399.9 eV, 400.8 eV and 401.3 eV (Fig. 4b) which can be assigned to lactam N [45], =NH and N—C=O groups [46], respectively. However, the 401.3 eV component can also be assigned to protonated amines [47], which are consistent with the zwitterionic nature of AMP [48]. Thus, since the Ti/TiO_2 surface is negatively charged [49], some electrostatic contributiontothe AMP- Ti/TiO_2 interactions cannot be discarded.

From the integrated signals of Ti 2p from the substrate and N 1s from the overlayer, and using the corresponding effective attenuation lengths [50] an AMP film thickness of 2 nm was estimated [51]. Considering the AMP density 0.8 g/cm^3 [52], the AMP surface concentration is about 0.16 μg/cm^2.

The S 2p signal (Fig. 4c) shows a doublet at 164 eV, which is consistent with free C—S bonds, that is, not linked to the surface [53], indicating that the sulfured moiety is not involved in the AMP-Ti/TiO_2 interaction.

3.3.2. AgNPs adsorption on Ti/TiO_2 surfaces

The adsorption of citrate-capped AgNPs on titanium surfaces has been previously explored by some of us [44]. The citrate-capped AgNPs are spontaneously immobilized on the Ti/TiO_2 surface through the interaction between the —OH groups from the surface and the $-COO^-$ groups from the citrate molecules, as it has been previously reported [44]. After 24 h immersion in the AgNPs dispersion, the substrates are totally covered by small islands, mainly

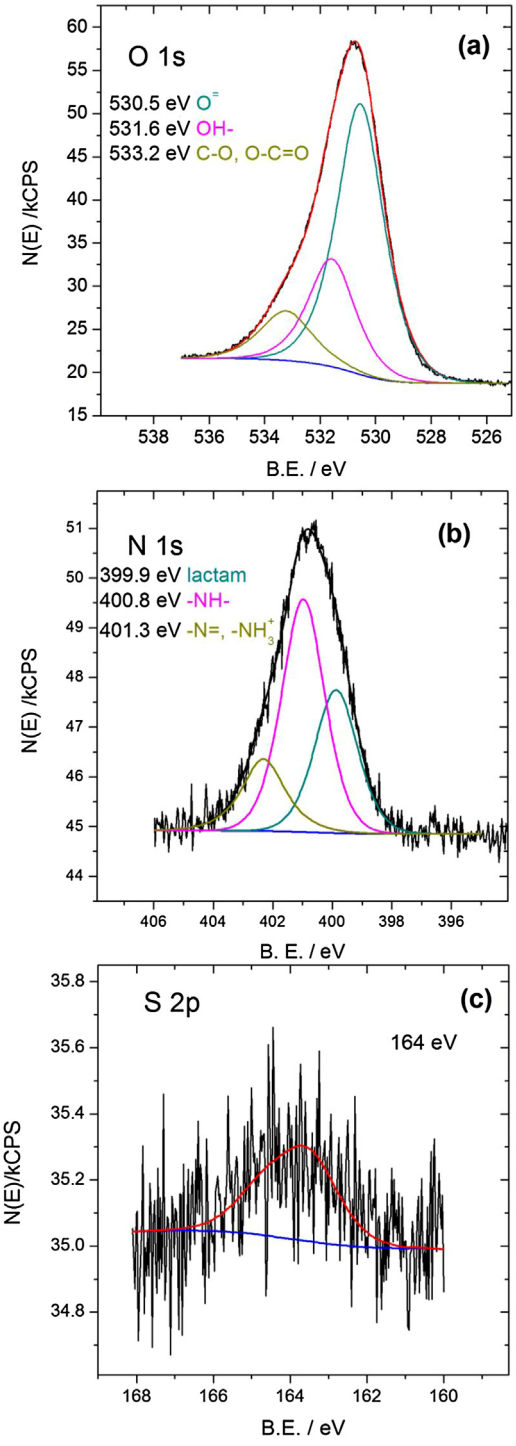

Fig. 4. XPS spectra of Ti-AMP surfaces. (a) O 1 s signal; (b) N 1 s signal; (c) S 2p signal.

consisting in aggregates (Fig. 5a), as it can be inferred from the cross section analysis of the AFM image (Fig. 5b). In fact, the observed aggregates have different heights, from 12 nm to 54 nm (Fig. 5c), indicating several layers of AgNPs, since the ~12 nm in height features are consistent with single silver nanoparticles, whereas higher features are compatible with stacked AgNPs. The surface concentration of AgNPs on the Ti substrates is 1.1 ± 0.2 μg/cm^2. The formation of aggregates in citrate-capped AgNPs has been attributed to nanoparticle–nanoparticle interactions stabilizing the islands. These interactions include van der Waals forces between

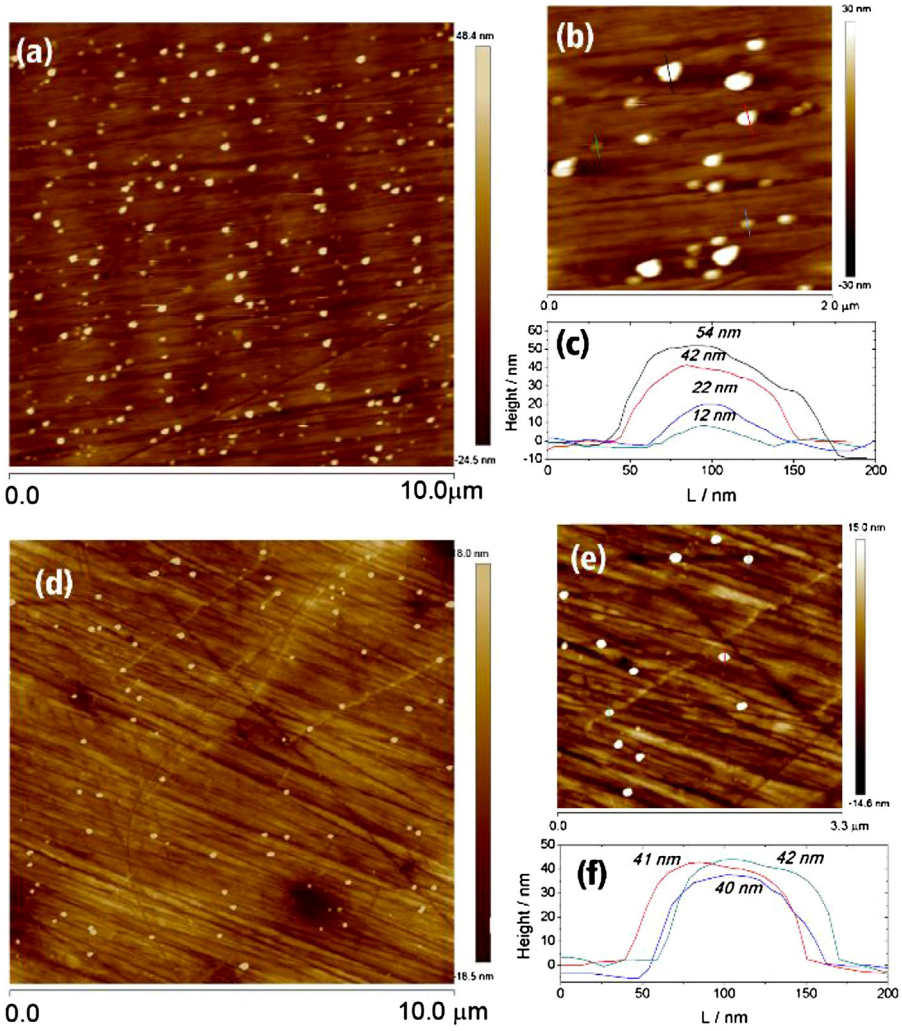

Fig. 5. (a) AFM image of Ti- AgNPs; (b) detail of image (a) showing the aggregates measured by cross sectional analysis (c); (d) AFM image of Ti-AgNPs/AMP; (e) detail of image (d) showing the aggregates measured by cross section analysis (f).

citrate chains and also hydrogen bonds [44], such as those proposed for the adsorption of gold nanoparticles on HOPG [54].

3.3.3. *AgNPs/AMP immobilization on the Ti/TiO_2 surface*

The AMP-modified AgNPs were successfully anchored on the Ti surface by simple immersion of the substrate in the AgNPs/AMP dispersion. According to the results described in the previous sections, the AMP would mediate the adsorption of AgNPs on the Ti substrates by means of S—Ag bonds involving the sulfured moiety of AMP and COOH— hidroxylated Ti/TiO_2 surfaces interactions. The change in the surface chemistry of the AgNPs when citrate is replaced with ampicillin results in smaller islands when compared to citrate-capped AgNPs adsorption as can be seen in Fig. 5d. Cross section analysis revealed almost uniform aggregates having about 40–43 nm in height (Fig. 5f). The formation of these aggregates would be promoted by capping–capping interactions and the following should be considered: on the one hand, AMP is a zwitterionic molecule, with the acid pK lower than the base pK; hence, the molecule is charged across the entire pH scale [48]. On this account, it might be possible that electrostatic interactions are responsible of the stabilization of the aggregates, since both the carboxylic acid and amino group in the zwitterionic capping are charged, yielding to electrostatic interactions between AMP/AgNPs. This mechanism has been proposed for cysteine-capped silver nanoparticles aggregation [55]. On the other hand, strong $\pi-\pi$ interactions are well known for being responsible for the stacking and packing of aromatic molecules. Thus, attractive non-bonded interactions between aromatic rings (labeled (7) in Fig. 1) either in off-centered parallel orientation or in T-shaped structure can also contribute to the overall attractive interactions among adsorbed AMP molecules [56]. Furthermore, Fig. 5d shows that AgNPs/AMP reaches a lower coverage than AgNPs (Fig. 5a). The percentage of covered surface calculated from AFM images is $4.4 \pm 0.2\%$ and $1.1 \pm 0.2\%$ for Ti-AgNPs and Ti-AgNPs/AMP respectively.

3.3.4. *Ti/TiO_2 with AgNPs and AMP multi-functionalization (Ti-AgNPs-AMP)*

The multi-functionalization was carried out in two steps. First, the substrates were exposed to the silver nanoprisms dispersion for 24 h. Then, the AgNPs-modified substrates were immersed in the AMP 24 h more.

As it was described above, the AMP molecule is adsorbed on titanium surface through strong interactions between the carboxylic group and the oxide on the surface, with some electrostatic interaction contribution. The sulfide moiety allows its immobilization on AgNPs. XPS analysis of the resulting surface after the two-steps functionalization confirms that AMP was adsorbed on both Ti/TiO_2 and AgNPs (Fig. 6).

As expected, the O 1s (Fig. 6a) and N 1s (Fig. 6b) spectra are similar to those described for AMP adsorption (see Section 3.3.1).

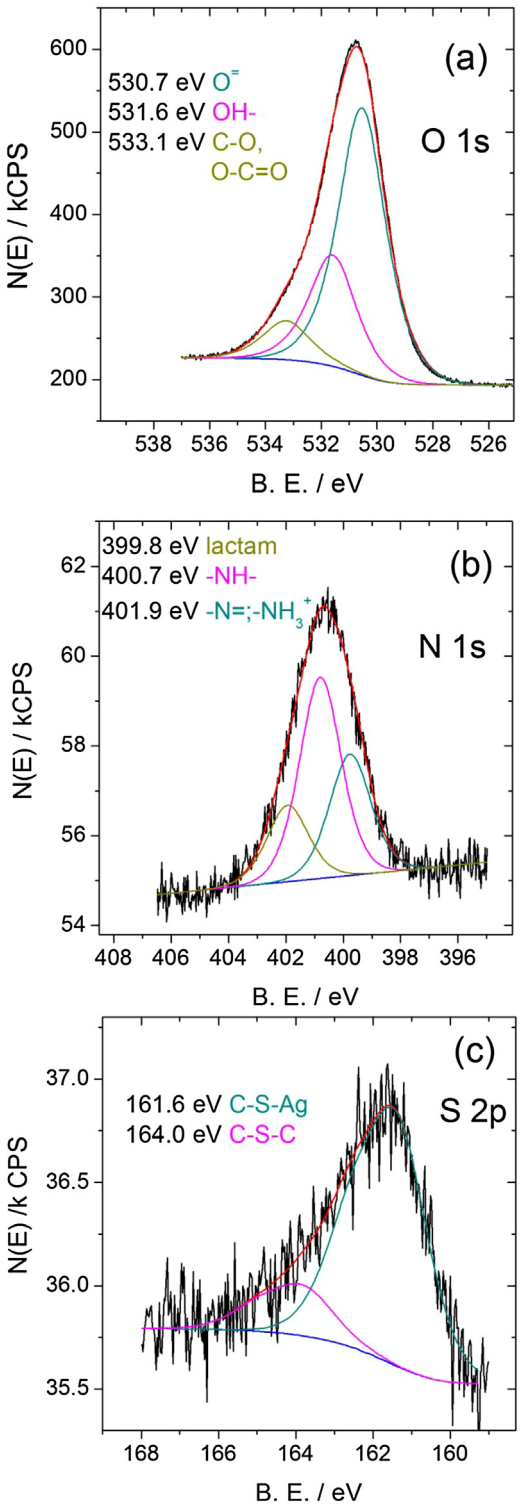

Fig. 6. XPS spectra of Ti-AgNPs-AMP surfaces. (a) O 1 s signal; (b) N 1 s signal; (c) S 2p signal.

It should be noted that, in this case, some signal from citrate molecules remaining on the AgNPs surface could contribute to the O 1s spectrum. What is certainly different from the spectra shown in Fig. 4 is the S 2p peak (Fig. 6c). In fact, the S 2p spectrum can be fitted with two doublets: the already found for AMP adsorption on TiO_2 at 164.0 eV, corresponding to free (not bonded to the surface) C—S—C portion of the molecule, and a second one at 161.6 eV. The last agrees with the widely accepted signal for chemisorbed S

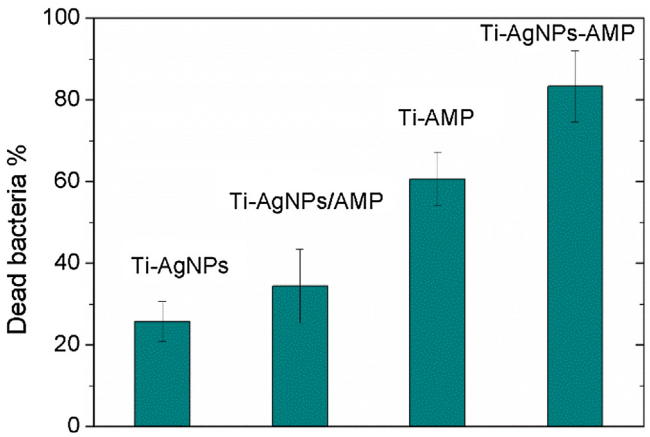

Fig. 7. Antibacterial effect of the modified substrates. The percentages were calculated with respect to a bare Ti surface (control).

forming thiolate bonds [57]. This result confirms those obtained by electrochemical assays previously described in this work (Section 3.3).

3.4. Functionalized surfaces antibacterial effect

The functionalized surfaces performance against *S. aureus* adhesion and proliferation was evaluated (Fig. 7). The dead bacteria percentage was calculated taking into account the proportion of viable bacteria on the modified-surfaces to viable bacteria on control (unmodified titanium substrate). Ti-AgNPs and Ti-AgNPs/AMP exhibit similar antibacterial activity (25.7 ± 4.9 and 34.4 ± 9.0%, respectively), which would indicate that AMP on the silver surface is not able to further decrease the number of viable bacteria.

The antibacterial action mechanism of AgNPs is still controversial. Among the proposed mechanisms, the most accepted ones involve Ag(I) ions release from the AgNPs, which interact with sulphur containing membrane proteins, generating physical damage to the membrane. Ag(I)-membrane proteins interactions may lead, in turn, to a drastic change in the membrane permeability, resulting in the dissipation of proton motive force and depletion of intracellular ATP levels. This may also elicit the intracellular accumulation of Ag(I) ions which can interfere with DNA replication or affect the respiratory chain. The toxicity effects of silver on microorganisms have also been ascribed to Ag(I) ions-related ROS production [58].

AMP immobilization on the AgNPs surface has been previously explored by other authors. However, unlike this work, these studies involve the dispersed in aqueous media AgNPs/AMP antimicrobial effect on planktonic cells. Brown et al. [33] synthesized monodispersed citrate-stabilized 4-nm silver nanoparticles which were later modified with AMP. These AMP-modified AgNPs displayed better antimicrobial activity against several bacterial strains than as synthesized AgNPs. They suggest that the antimicrobial activity of functionalized AgNP/AMP resides in the combined activity of AgNP and the ampicillin carried on the surface of the nanoparticle. On the other hand, Hur et al. [59] were able to functionalize AgNPs with AMP in a one-step procedure in which AMP was also used as a reducing agent. Among the tested Gram-positive and Gram-negative bacteria, the newly prepared NPs show the highest antibacterial activities against *Streptococcus pyogenes*. Unlike these observations, in this work, AgNPs and AgNPs/AMP immobilized on the surface showed a similar antibacterial effect on *S. aureus*. This apparent discrepancy can be explained considering that the coverage of AgNPs/AMP is lower than AgNPs, as it was already described in Section 3.3.3. In addition to the lower coverage, AgNPs/AMP aggregates are smaller than the AgNPs ones. However, the capacity

of both surfaces to inhibit the bacterial growth is similar, indicating that the lower coverage of silver on Ti- AgNPs/AMP is compensated by the enhanced antimicrobial activity of the antibiotic-modified AgNPs. It is worth noting that the β-lactam ring in penicillin-type antibiotics interferes in the synthesis of the bacterial cell wall by binding to specific penicillin-binding proteins (PBPs) located inside the cell wall, hence leading to the death of the bacterial cell due to either osmotic instability or cell lysis. Since AMP is adsorbed on the silver surface through a thiolate bond, the β-lactam ring is free to interact with the cell. Consequently, the mechanism involving antibacterial activity of AgNPs/AMP would include the action of β-lactam ring on the cell wall (first level, death by contact) and also Ag(I) release (second level, death by release), supporting the observation of an enhanced antibacterial effect.

On the other hand, on Ti-AMP substrates, the proportion of dead bacteria reaches the 60.6 ± 6.6% (Fig. 7). Since the antibiotic binds to the Ti/TiO_2 surface via the carboxyl group, the lactam group is able to interact with the cell wall of the attached bacteria and then prevent cell proliferation.

Among the substrates assayed, the multi-functionalized Ti-AgNPs-AMP samples exhibit the best bactericidal activity, since the 83.3 ± 8% of cells attached to these surfaces are dead. These multi-functionalized substrates were prepared by a two-step procedure: in the first step, the adsorption of the as synthesized AgNPs leads to a substrate having the highest amount of silver which can be reached under the experimental conditions used in this work. In the second step, AMP immobilization occurs on both Ti/TiO_2 and Ag surfaces. Therefore, the surface concentration of both AgNPs and AMP in the substrates thus obtained is higher than that corresponding to AgNPs/AMP. On the other hand, comparing Ti-AMP and the multi-functionalized surfaces performance, it is straightforward that AgNPs act as an extra-source of bactericidal agent. As a result, the combination of the two agents having different targets, which can overcome the bacterial mechanism of resistance, leads to an enhanced inhibition of cell proliferation. It is worth mentioning that "antimicrobial surfaces" accounts for those surfaces which work to prevent or limit the growth and proliferation of bacteria [60]. This is an important distinction, as the word "antibacterial" is usually understood as being effective in killing bacterial cells. Therefore, the surfaces described in this work fall under the definition of "antibacterial". Interestingly, the multi-functionalized surface seems to be a good candidate for long term treatments, such as those required in indwelling devices, since, as mentioned before, the two antibacterial agents anchored on this surface have different kinetics: AMP effect occur by contact at the early stages of bacterial proliferation, while AgNPs behave as a silver reservoir, since Ag(I) ions release is not immediate, but rather progressive. Consequently, in order to evaluate if all the assayed surfaces keep their performance over time, we have emulated the elapsed time by re-using the surfaces, which represents the most unfavorable situation, since a new refreshed set of sessile *S. aureus* was challenged at each re-utilization time.

3.5. Antibacterial effect over time

We have emulated the performance of the surfaces over time, by testing the viability of sessile cells after re-using the substrates as described below.

The Ti-AgNPs, Ti-AMP and Ti-AgNPs-AMP surfaces were exposed to the bacterial suspension for 2 h to allow bacterial adhesion, and then the number of viable bacteria was determined. This first colonization and viable bacteria count defined time T1. After determining the number of viable cells, these functionalized surfaces exposed to bacteria for a second stage of colonization defined T2. Finally, these surfaces were exposed to a last stage of colonization and viable bacteria count defined as T3. Therefore, the times

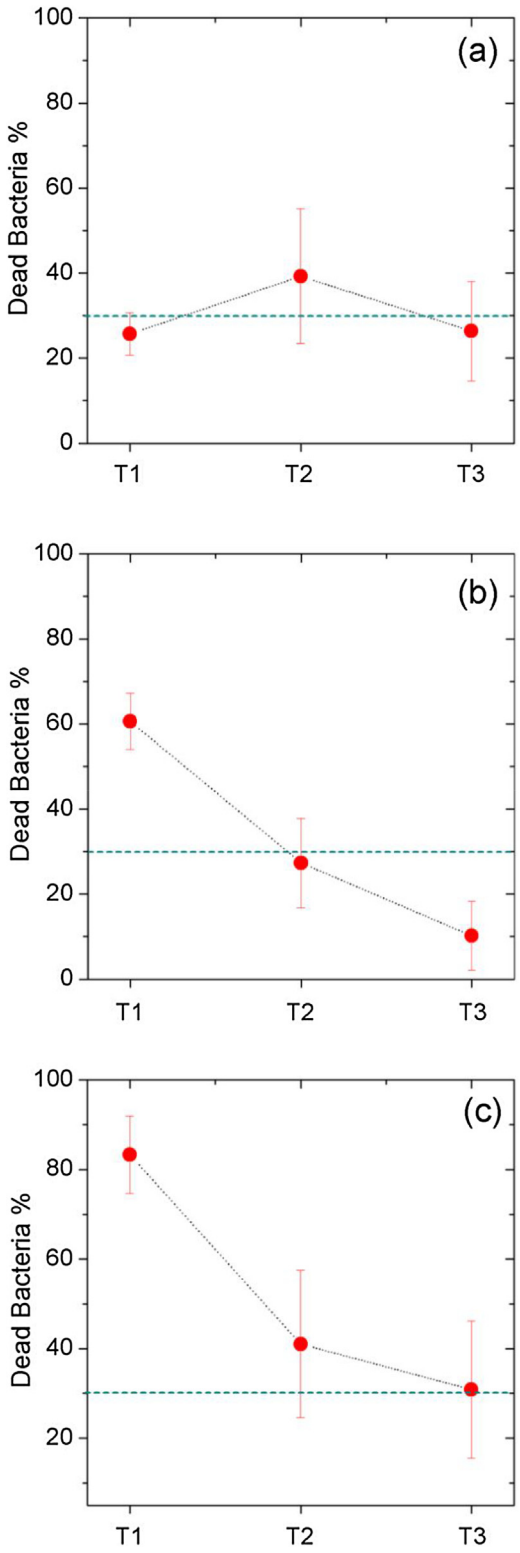

Fig. 8. Viable bacteria after the reutilization of the modified titanium substrates. (a) Ti-AgNPs; (b) Ti-AMP; (c) multi-functionalized Ti-AgNPs-AMP. The horizontal dotted line points out the average dead bacteria for Ti-AgNPs.

T1, T2 and T3 correlate with the number of re-utilization. It should be noticed that we considered the most unfavorable situation, i.e., a new refreshed set of sessile *S. aureus* was challenged at each re-utilization time.

Fig. 8 shows the dead bacteria on all the surfaces for T1, T2 and T3. The Ti-AgNPs substrate (Fig. 8a) keeps its bactericidal effect

around 30%, indicating a similar Ag(I) ions release at each step. On the Ti-AMP substrates, the relatively high initial efficiency for killing cells (T1) drops to less than a half in the second experiment (T2), reaching the lowest effect after the third use (T3), since almost 90% of cells remain viable. As regards, it should be taken into account that the β-lactam group functionality in the ampicillin molecule is not recovered after binding to PBPs, yielding to a decrease in the functional β-lactam ring surface concentration and, hence, to a reduced capacity for causing a decrease in the bacterial viability.

The multi-functionalized surface bactericidal activity is shown in Fig. 8c. As expected, the highest effect is found on this surface at the first stage of bacterial colonization due to the combined action of AMP and Ag(I) ions. After T2, the ability for killing cells decreases as a consequence of AMP functionality loss. At this step, the main contribution to cell growth inhibition came from Ag(I) ions release. Finally, at T3, the number of unviable bacteria on the surface reaches a constant value, which is similar to that found for Ti-AgNPs, supporting the idea that AgNPs behave as a reservoir for a progressive Ag(I) ions release to the media. In fact, we have measured the amount of Ag(I) ions released to SSF after 6 h immersion (which correspond to 3 immersion cycles in culture media, T3), and after 24 h immersion, which correspond to longer times. SSF was chosen taking into account that the intended application of the designed surfaces is avoiding infections in orthopedic devices, including dental implants. These experiments lead to $0.15 \pm 0.09\ \mu g/cm^2$ and $0.27 \pm 0.09\ \mu g/cm^2$ after 6 h and 24 h, respectively. Notice that Ag(I) ions released from the surface are able to interact with proteins in biological media via carboxylate and thiol groups and also could be separate from the solution by silver chloride and/or silver phosphate salt formation and precipitation. However, our results indicate that even though the Ag(I) concentration may be reduced in biological fluids, the amount of silver released to the liquid environmentis high enough to sustain the bacteriostatic effect over time. Therefore, the multi-functionalized surface is a good candidate for preventing infections in implantable devices, since it is able to reduce the 83% of viable bacteria at the first stages of implantation when bacteria would have the highest growth rate, helping the action of the immune system and the conventional dose of oral antibiotics.

4. Conclusions

The development of a simple two-steps protocol to prepare surfaces able to keep the antibacterial capacity over time through the multi-functionalization of Ti surfaces was successfully achieved. Since no previous surface conditioning is required, this method is easy and inexpensive, and do not require special equipment and/or trained lab specialists. Two antimicrobial agents, the β-lactam ampicillin and silver nanoparticles, having different mechanisms of action were immobilized on Ti/TiO_2 surfaces. AMP adsorption onthe Ti/TiO_2 surface was reached by simple immersion of the substrate in the AMP solution. The antibiotic binds to the surface through covalent interactions between the —COOH groups in AMP and the —OH groups on the surface, although the contribution of some electrostatic interactions between the protonated amine in AMP and the negatively charged Ti/TiO_2 surface cannot be discarded. The antibiotic anchoring to the AgNPs is carried out by thiolate-like bonds, as it has been demonstrated in this work by electrochemical and XPS analysis. To the best of our knowledge, the interactions involved in the penicillin-type antibiotics immobilization on silver and titanium surfaces have not been previously reported, thus establishing the basis for the further anchoring of other antibacterial compounds having similar functional groups.

In order to find a surface able to produce the best antibacterial behavior, we have tested the performance of Ti-AgNPs, Ti-AgNPs/AMP, Ti-AMP and Ti-AgNPs-AMP against *S. aureus* sessile cells. Ti-AMP and Ti-AgNPs-AMP showed the highest antibacterial effect, indicating that the β-lactam ring functionality is maintained after the adsorption process. Moreover, the antimicrobial capacity is maintained over time due to a two-pathway antibacterial action mechanism: death by contact (AMP) and death by release (AgNPs). The effect of AMP prevails on AgNPs at early stages of bacterial adhesion, while AgNPs are responsible for sustaining the relatively low but steady release of Ag(I). This behavior would preserve the bacteriostatic activity of the surface over time and, thus, would contribute to preventing infections due to sessile cells on indwelling devices, powering the action of the immune system and the conventional antibiotics usually dosed in implanted patients.

Acknowledgements

We gratefully acknowledge CONICET (PIP 112-201501-00601CO) and UNLP (Projects 11/X665 and 11/X760). The authors are grateful to Dr. Lia Pietrasanta and Centro de Microscopías Avanzadas (UBA) for the TEM image. We also thank Dr. Roberto C. Salvarezza for his helpful discussions.

References

[1] A.J. Tande, R. Patel, Prosthetic joint infection, Clin. Microbiol. Rev. 27 (2014) 302–345, http://dx.doi.org/10.1128/CMR.00111-13.
[2] M. Villanueva, Infección de Prótesis total de rodilla y cadera, http://doctorvillanueva.com/especialidades/protesis-de-rodilla/infeccion-de-protesis-total-de-rodilla-y-cadera/, http://doctorvillanueva.com/especialidades/protesis-de-Rodilla/infeccion-de-Protesis-Total-de-Rodilla-Y-Cadera/.
[3] J.W. Costerton, Bacterial biofilms a common cause of persistent infections, Science (80-) 284 (1999) 1318–1322, http://dx.doi.org/10.1126/science.284.5418.1318.
[4] M.T. Butler, Q. Wang, R.M. Harshey, Cell density and mobility protect swarming bacteria against antibiotics, Proc. Natl. Acad. Sci. U. S. A. 107 (2010) 3776–3781, http://dx.doi.org/10.1073/pnas.0910934107.
[5] N. Aumsuwan, S. Heinhorst, M.W. Urban, The effectiveness of antibiotic activity of penicillin attached to expanded poly(tetrafluoroethylene) (ePTFE) surfaces: a quantitative assessment, Biomacromolecules 8 (2007) 3525–3530, http://dx.doi.org/10.1021/bm700803e.
[6] N. Aumsuwan, S. Heinhorst, M.W. Urban, Antibacterial surfaces on expanded polytetrafluoroethylene; penicillin attachment, Biomacromolecules 8 (2007) 713–718, http://dx.doi.org/10.1021/bm061050k.
[7] N. Aumsuwan, R.C. Danyus, S. Heinhorst, M.W. Urban, Attachment of ampicillin to expanded poly(tetrafluoroethylene): surface reactions leading to inhibition of microbial growth, Biomacromolecules 9 (2008) 1712–1718, http://dx.doi.org/10.1021/bm800176t.
[8] W.-S. Bae, M.W. Urban, Creating patterned poly(dimethylsiloxane) surfaces with amoxicillin and poly(ethylene glycol), Langmuir 22 (2006) 10277–10283, http://dx.doi.org/10.1021/la061571t.
[9] B.M. Beadle, R.A. Nicholas, B.K. Shoichet, Interaction energies between beta-lactam antibiotics and E. coli penicillin-binding protein 5 by reversible thermal denaturation, Protein Sci. 10 (2001) 1254–1259, http://dx.doi.org/10.1110/ps.52001.
[10] J.C. Love, L.A. Estroff, J.K. Kriebel, R.G. Nuzzo, G.M. Whitesides, Self-assembled monolayers of thiolates on metals as a form of nanotechnology, Chem. Rev. 105 (2005) 1103–1169, http://dx.doi.org/10.1021/cr0300789.
[11] Antimicrobial Resistance. Global Report Onsurveillance, World Health Organization, 2014, Fact sheet N°194 Updated April 2015.
[12] A. D'Agostino, A. Taglietti, P. Grisoli, G. Dacarro, L. Cucca, M. Patrini, P. Pallavicini, Seed mediated growth of silver nanoplates on glass: exploiting the bimodal antibacterial effect by near IR photo-thermal action and Ag^+ release, RSC Adv. 6 (2016) 70414–70423, http://dx.doi.org/10.1039/C6RA11608F.
[13] A. D'Agostino, A. Taglietti, R. Desando, M. Bini, M. Patrini, G. Dacarro, L. Cucca, P. Pallavicini, P. Grisoli, Bulk surfaces coated with triangular silver nanoplates: antibacterial action based on silver release and photo-thermal effect, Nanomaterials 7 (2017) 7, http://dx.doi.org/10.3390/nano7010007.
[14] E. Amato, Y.A. Diaz-Fernandez, A. Taglietti, P. Pallavicini, L. Pasotti, L. Cucca, C. Milanese, P. Grisoli, C. Dacarro, J.M. Fernandez-Hechavarria, V. Necchi, Synthesis, characterization and antibacterial activity against gram positive and gram negative bacteria of biomimetically coated silver nanoparticles, Langmuir 27 (2011) 9165–9173, http://dx.doi.org/10.1021/la201200r.
[15] H. Lara, N. Ayala-Núñez, L. Ixtepan Turrent, C. Rodríguez Padilla, Bactericidal effect of silver nanoparticles against multidrug-resistant bacteria, World J.

Microbiol. Biotechnol. 26 (2010) 615–621, http://dx.doi.org/10.1007/s11274-009-0211-3.
[16] N. Duran, M. Duran, M.B. de Jesus, A.B. Seabra, W.J. Favaro, G. Nakazato, Silver nanoparticles: a new view on mechanistic aspects on antimicrobial activity, Nanotechnol. Biol. Med. 12 (2016) 789–799, http://dx.doi.org/10.1016/j.nano.2015.11.016.
[17] S. Prabhu, E.K. Poulose, Silver nanoparticles: mechanism of antimicrobial action, synthesis, medical applications, and toxicity effects, Int. Nano Lett. 2 (2012) 32, http://dx.doi.org/10.1186/2228-5326-2-32.
[18] W.-R. Li, X.-B. Xie, Q.-S. Shi, H.-Y. Zeng, Y.-S. Ou-Yang, Y.-B. Chen, Antibacterial activity and mechanism of silver nanoparticles on Escherichia coli, Appl. Microbiol. Biotechnol. 85 (2010) 1115–1122, http://dx.doi.org/10.1007/s00253-009-2159-5.
[19] K.B. Holt, A.J. Bard, Interaction of Silver(I) ions with the respiratory chain of escherichia coli: an electrochemical and scanning electrochemical microscopy study of the antimicrobial mechanism of micromolar Ag+, Biochemistry 44 (2005) 13214–13223, http://dx.doi.org/10.1021/bi0508542.
[20] X. Li, J.J. Lenhart, Aggregation and dissolution of silver nanoparticles in natural surface water, Environ. Sci. Technol. 46 (2012) 5378–5386, http://dx.doi.org/10.1021/es204531y.
[21] S. Sivolella, E. Stellini, G. Brunello, C. Gardin, L. Ferroni, E. Bressan, B. Zavan, Silver nanoparticles in alveolar bone surgery devices, J. Nanomater. 2012 (2012), http://dx.doi.org/10.1155/2012/975842, 12 pages.
[22] G.A. Sotiriou, S.E. Pratsinis, Antibacterial activity of nanosilver ions and particles, Environ. Sci. Technol. 44 (2010) 5649–5654, http://dx.doi.org/10.1021/es101072s.
[23] A. Taglietti, Y.A. Diaz Fernandez, E. Amato, L. Cucca, G. Dacarro, P. Grisoli, V. Necchi, P. Pallavicini, L. Pasotti, M. Patrini, Antibacterial activity of glutathione-Coated silver nanoparticles against gram positive and gram negative bacteria, Langmuir 28 (2012) 8140–8148, http://dx.doi.org/10.1021/la3003838.
[24] J. Wu, S. Hou, D. Ren, P.T. Mather, Antimicrobial properties of nanostructured hydrogel webs containing silver, Biomacromolecules 10 (2009) 2686–2693, http://dx.doi.org/10.1021/bm900620w.
[25] Z. Xiu, Q. Zhang, H.L. Puppala, V.L. Colvin, P.J.J. Alvarez, Negligible particle-specific antibacterial activity of silver nanoparticles, Nano Lett. 12 (2012) 4271–4275, http://dx.doi.org/10.1021/nl301934w.
[26] E.T. Hwang, J.H. Lee, Y.J. Chae, Y.S. Kim, B.C. Kim, B.I. Sang, M.B. Gu, Analysis of the toxic mode of action of silver nanoparticles using stress-specific bioluminescent bacteria, Small 4 (2008) 746–750, http://dx.doi.org/10.1002/smll.200700954 http://www.scopus.com/inward/record.url?eid=2-s2.0-47549114699&partnerID=40&md5=8454f471e4ff7c52d2f1e12bc62eb422.
[27] C. Levard, E.M. Hotze, G.V. Lowry, G.E. Brown, Environmental transformations of silver nanoparticles: impact on stability and toxicity, Environ. Sci. Technol. 46 (2012) 6900–6914, http://dx.doi.org/10.1021/es2037405.
[28] Q.L. Feng, J. Wu, G.Q. Chen, F.Z. Cui, T.N. Kim, J.O. Kim, A mechanistic study of the antibacterial effect of silver ions on Escherichia coli and Staphylococcus aureus, J. Biomed. Mater. Res. 52 (2000) 662–668, http://dx.doi.org/10.1002/1097-4636(20001215)52:4<662:aid-jbm10>3.0.co;2-3.
[29] Y. Oshida, Bioscience and Bioengineering of Titanium Materials, 2nd ed., Elsevier Ltd, 2013, http://dx.doi.org/10.1016/B978-0-444-62625-7.00008-X.
[30] B. Feng, J.Y. Chen, S.K. Qi, L. He, J.Z. Zhao, X.D. Zhang, Characterization of surface oxide films on titanium and bioactivity, J. Mater. Sci. Mater. Med. 13 (2002) 457–464, http://dx.doi.org/10.1023/A:1014737831371.
[31] S. Schroth, M. Schneider, T. Mayer – Uhma, A. Michaelis, V. Klemm, Investigation of thin oxide films on titanium for capacitor applications, Surf. Interface Anal. 40 (2008) 850–852, http://dx.doi.org/10.1002/sia.2708.
[32] A.J. Frank, N. Cathcart, K.E. Maly, V. Kitaev, Synthesis of silver nanoprisms with variable size and investigation of their optical properties: a first-year undergraduate experiment exploring plasmonic nanoparticles, J. Chem. Educ. 87 (2010) 1098–1101, http://dx.doi.org/10.1021/ed100166g.
[33] A.N. Brown, K. Smith, T.A. Samuels, J. Lu, S.O. Obare, M.E. Scott, Nanoparticles functionalized with ampicillin destroy multiple-antibiotic-resistant isolates of Pseudomonas aeruginosa and Enterobacter aerogenes and methicillin-resistant Staphylococcus aureus, Appl. Environ. Microbiol. 78 (2012) 2768–2774, http://dx.doi.org/10.1128/AEM.06513-11.
[34] S. Bandari, V.R. Dronam, B.B. Eedara, Development and preliminary characterization of levofloxacin pharmaceutical cocrystals for dissolution rate enhancement, J. Pharm. Invest. 47 (2017) 583–591, http://dx.doi.org/10.1007/s40005-016-0302-8.
[35] C.Y. Flores, A.G. Miñán, C.A. Grillo, R.C. Salvarezza, C. Vericat, P.L. Schilardi, Citrate-capped silver nanoparticles showing good bactericidal effect against both planktonic and sessile bacteria and a low cytotoxicity to osteoblastic cells, Appl. Mater. Interfaces 5 (2013) 3149–3159, http://dx.doi.org/10.1021/am400044e http://www.scopus.com/inward/record.url?eid=2-s2.0-84876726820&partnerID=40&md5=563be723b490ff8f26d6389af201961e.
[36] S. Kaniyankandy, J. Nuwad, C. Thinaharan, G.K. Dey, C.G.S. Pillai, Electrodeposition of silver nanodendrites, Nanotechnology 18 (2007) 125610, http://dx.doi.org/10.1088/0957-4484/18/12/125610.
[37] V. Brunetti, B. Blum, R.C. Salvarezza, A.J. Arvia, Comparative molecular resolution STM imaging of thiourea, ethylthiourea, and sulfur self-assembled adlayer structures on silver (111), Langmuir 19 (2003) 5336–5343, http://dx.doi.org/10.1021/la034005w.
[38] O. Azzaroni, M.E. Vela, G. Andreasen, P. Carro, R.C. Salvarezza, Electrodesorption potentials of self-assembled alkanethiolate monolayers on Ag(111) and Au(111). An electrochemical, scanning tunneling microscopy and density functional theory study, J. Phys. Chem. B 106 (2002) 12267–12273, http://dx.doi.org/10.1021/jp0219653.
[39] K. Arihara, T. Ariga, N. Takashima, K. Arihara, T. Okajima, F. Kitamura, K. Tokuda, T. Ohsaka, Multiple voltammetric waves for reductive desorption of cysteine and 4-mercaptobenzoic acid monolayers self-assembled on gold substrates, Phys. Chem. Chem. Phys. 5 (2003) 3758, http://dx.doi.org/10.1039/b305867k.
[40] Y. Luo, J. Luo, W. Zhou, X. Qi, H. Zhang, D.Y.W. Yu, C.M. Li, H.J. Fan, T. Yu, Controlled synthesis of hierarchical graphene-wrapped TiO 2 @Co 3 O 4 coaxial nanobelt arrays for high-performance lithium storage, J. Mater. Chem. A 1 (2013) 273–281, http://dx.doi.org/10.1039/C2TA00064D.
[41] H. Onishi, Carboxylates Adsorbed on TiO2 (110), Springer, Berlin Heidelberg, 2003, pp. 75–89, http://dx.doi.org/10.1007/978-3-662-05250-1_5.
[42] A. Sasahara, H. Uetsuka, H. Onishi, Image topography of alkyl-substituted carboxylates observed by noncontact atomic force microscopy, Surf. Sci. 481 (2001) L437–L442, http://dx.doi.org/10.1016/S0039-6028(01)01028-7.
[43] B.-X. Zhang, G.-Y. Zhang, H. Gao, S.-H. Wu, J.-H. Chen, X.-L. Li, One-step hydrothermal synthesis and optical properties of PEG-passivated nitrogen-doped carbon dots, RSC Adv. 5 (2015) 7395–7400, http://dx.doi.org/10.1039/C4RA08869G.
[44] C.Y. Flores, C. Diaz, A. Rubert, G.A. Benítez, M.S. Moreno, M.A. Fernández Lorenzo de Mele, R.C. Salvarezza, P.L. Schilardi, C. Vericat, Spontaneous adsorption of silver nanoparticles on Ti/TiO2 surfaces. Antibacterial effect on Pseudomonas aeruginosa, J. Colloid Interface Sci. 350 (2010) 402–408, http://dx.doi.org/10.1016/j.jcis.2010.06.052 http://www.sciencedirect.com/science/article/B6WHR-50CVR24-2/2/7edc6329156f616daa04d8d5b42e6eb9.
[45] B.-X. Zhang, G.-Y. Zhang, H. Gao, S.-H. Wu, J.-H. Chen, X.-L. Li, One-step hydrothermal synthesis and optical properties of PEG-passivated nitrogen-doped carbon dots, RSC Adv. 5 (2015) 7395–7400, http://dx.doi.org/10.1039/C4RA08869G.
[46] Hyung Jin Kim, In-Seob Bae, Sang-Jin Cho, Jin-Hyo Boo, Byung-Cheo Lee, Jinhee Heo, Ilsub Chung, Byungyou Hong, Synthesis and characteristics of NH2-functionalized polymer films to align and immobilize DNA molecules, Nanoscale Res. Lett. 7 (2012) 30–37, http://dx.doi.org/10.1209/epl/i2001-00412-2.
[47] A. Cossaro, M. Dell'Angela, A. Verdini, M. Puppin, G. Kladnik, M. Coreno, M. de Simone, A. Kivimäki, D. Cvetko, M. Canepa, L. Floreano, Amine functionalization of gold surfaces: ultra high vacuum deposition of cysteamine on Au(111), J. Phys. Chem. C 114 (2010) 15011–15014, http://dx.doi.org/10.1021/jp104824c.
[48] J.E.A. Comer, Ionization constants and ionization profile, in: B. Testa (Ed.), Compr. Med. Chem., vol. II, Elsevier Ltd, 2007, pp. 357–397, http://dx.doi.org/10.1016/B0-08-045044-X/00133-4.
[49] D.J. Gorth, S. Puckett, B. Ercan, T.J. Webster, M. Rahaman, B. Sonny Bal, Decreased bacteria activity on Si_3N_4 surfaces compared with PEEK or titanium, Int. J. Nanomed. 7 (2012) 4829–4840, http://dx.doi.org/10.2147/IJN.S35190 http://www.scopus.com/inward/record.url?eid=2-s2.0-84870384050&partnerID=40&md5=48d8933f627196679e3f64e56f9c550b.
[50] M.P. Seah, Simple universal curve for the energy-dependent electron attenuation length for all materials, Surf. Interface Anal. 44 (2012) 1353–1359, http://dx.doi.org/10.1002/sia.5033.
[51] P.J. Cumpson, The Thickogram: a method for easy film thickness measurement in XPS, Surf. Interface Anal. 29 (2000) 403–406, http://dx.doi.org/10.1002/1096-9918(200006)29:6<403:AID-SIA884>3.0.CO;2-8.
[52] http://www.chemicalland21.com/lifescience/phar/AMPICILLIN.htm, Ampicillin.
[53] A. Guarnaccio, M. D'Auria, R. Racioppi, G. Mattioli, A.A. Bonapasta, A. De Bonis, R. Teghil, K.C. Prince, R.G. Acres, A. Santagata, Thiophene-based oligomers interacting with silver surfaces and the role of a condensed benzene ring, J. Phys. Chem. C 120 (2016) 252–264, http://dx.doi.org/10.1021/acs.jpcc.5b08733.
[54] D. Grumelli, C. Vericat, G. Benitez, M.E. Vela, R.C. Salvarezza, L.J. Giovanetti, J.M. Ramallo-López, F.G. Requejo, A.F. Craievich, Y.S. Shon, Thiol-capped gold nanoparticles on graphite: spontaneous adsorption and electrochemically induced release, J. Phys. Chem. C 111 (2007) 7179–7184, http://dx.doi.org/10.1021/jp071357t.
[55] H.S. Toh, C. Batchelor-Mcauley, K. Tschulik, R.G. Compton, Chemical interactions between silver nanoparticles and thiols: a comparison of mercaptohexanol against cysteine, Sci. China Chem. 57 (2014) 1199–1210, http://dx.doi.org/10.1007/s11426-014-5141-8.
[56] G.B. McGaughey, M. Gagné, A.K. Rappé, pi-Stacking interactions. Alive and well in proteins, J. Biol. Chem. 273 (1998) 15458–15463, http://dx.doi.org/10.1074/JBC.273.25.15458.
[57] C. Vericat, M.E. Vela, G. Benitez, P. Carro, R.C. Salvarezza, Self-assembled monolayers of thiols and dithiols on gold: new challenges for a well-known system, Chem. Soc. Rev. 39 (2010) 1805–1834, http://dx.doi.org/10.1039/b907301a.
[58] S. Chernousova, M. Epple, Silver as antibacterial agent: ion, nanoparticle, and metal, Angew. Chem. Int. Ed. 52 (2013) 1636–1653, http://dx.doi.org/10.1002/anie.201205923.
[59] Y.E. Hur, S. Kim, J.H. Kim, S.H. Cha, M.J. Choi, S. Cho, Y. Park, One-step functionalization of gold and silver nanoparticles by ampicillin, Mater. Lett. 129 (2014) 185–190, http://dx.doi.org/10.1016/j.matlet.2014.05.032.
[60] E. Ivanova, R. Crawford (Eds.), Antibacterial Surfaces, Springer International Publishing, Cham, 2015, http://dx.doi.org/10.1007/978-3-319-18594-1.